International Journal of Pharmaceutics 388 (2010) 1–12

Contents lists available at ScienceDirect

International Journal of Pharmaceutics

journal homepage: www.elsevier.com/locate/ijpharm

The interplay of membrane formation and drug release in solution-cast films of polylactide polymers

Decheng Ma[1], Anthony J. McHugh*

Department of Chemical Engineering, Lehigh University, 111 Research Drive, Bethlehem, PA 18015, United States

ARTICLE INFO

Article history:
Received 10 September 2009
Received in revised form 7 December 2009
Accepted 10 December 2009
Available online 16 December 2009

Keywords:
Membrane
Phase inversion
Controlled release
Biodegradable
Drug delivery

ABSTRACT

The interplay of phase inversion and drug release has been studied for films of several biodegradable polylactide polymers cast from solutions containing polymer, solvent, and drug (naproxen). Variables studied included polymer type and concentration, solvent type, and film casting conditions (i.e. free or forced convection, humidity). Film morphologies and thermal properties indicate that reduction of the T_g of the amorphous poly (lactide-*co*-glycolide) (PLGA) and poly (D, L-lactide) (PDLLA) systems caused by the drug, inhibits stabilization of a porous, structure, regardless of dry casting conditions and drug loads. Porous membranes could be formed by wet casting; however, drug loss during casting, makes this a non-viable process. For semi-crystalline PLLA, membrane morphologies could be varied by controlling the mass transfer path to form a single-phase dense film by polymer crystallization or a liquid–liquid two-phase structure followed by locking-in by polymer crystallization. However, the lack of drug solubility in the crystalline phase leads to unfavorable drug distributions most often leading to a burst release. Release profiles for all three polymers were found to follow a two-stage release model, with a first stage diffusive release followed by zero-order release in the second stage due to polymer erosion.

1. Introduction

Studies in our laboratory have shown that the drug release characteristics of solution-cast films of relatively high glass transition polymers [cellulose acetate (CA) (Ma and McHugh, 2007) and poly (*n*-butyl cyanoacrylate) (PBCA) (Xiang et al., submitted for publication)] are profoundly influenced by the casting conditions and morphologies that form during phase inversion. Since CA is non-degradable and PBCA, although degradable, remains stable on the time scales of the film formation-release experiments (Xiang et al., submitted for publication), the impact of film morphology on the drug release kinetics can be isolated for both systems. A key feature is the interplay between the plasticizing effects of the drug, its crystallization rate, and the mass transfer dynamics during quenching that promote locking-in of the phase-separated membrane structure. As a result of this interplay, porous morphologies that encapsulate the drug in the body of the film can be produced at high drug load (DL), with minimal bursting on release.

We have recently extended our studies to include several commonly used amorphous and crystallizable biodegradable polymers, including amorphous copolymer poly (lactide-*co*-glycolide) (PLGA), single, amorphous poly (D, L-lactide) (PDLLA), crystallizable poly (L-lactide) (PLLA) and poly (ε-caprolactone) (PCL) and blends therein, with naproxen as the active pharmaceutical agent. Although these polymers have been used broadly in drug delivery areas (Brodbeck et al., 1999; Mohamed and van der Walle, 2008; Stamatialis et al., 2008), to our knowledge, the role of polymer–drug interactions and phase inversion dynamics in the formation of their membrane morphologies and associated drug release behavior have not been systematically studied. In this study, membrane morphologies, and drug–polymer interactions will be shown to have a dramatic effect on the drug release kinetics.

2. Experimental

2.1. Materials

The poly (D, L-lactide-*co*-glycolide) (50/50, IV 0.58 dL/g in HFIP), poly (D, L-lactide) (IV 0.66 dL/g in chloroform), and poly (L-lactide) (IV 0.99 dL/g in chloroform) used in these studies were purchased from Durect (Pelham, AL). Poly (ε-caprolactone) (M_w ~80,000 GPC), acetone, dichloromethane, tetrahydrofuran (THF), dioxane, chloroform, and (*S*)-(+)-6-methoxy-α-methyl-2-naphthaleneacetic acid (naproxen, 98%), were obtained from Aldrich (St. Louis, MO). Acetonitrile, methanol, ethanol, and *o*-phosphoric acid (85%, HPLC grade) were purchased from Fisher (Fairlawn, NJ). All solvents were HPLC grade, and all chemicals were used without further

* Corresponding author. Tel.: +1 610 758 4470; fax: +1 610 758 6245.
E-mail address: ajm8@lehigh.edu (A.J. McHugh).
[1] Current address: Merck & Co., Inc., West Point, PA 19486, United States.

0378-5173/$ – see front matter © 2009 Elsevier B.V. All rights reserved.
doi:10.1016/j.ijpharm.2009.12.027

purification. Water (de-ionized, DI) was prepared with Millipore Milli-Q® system (Billerica, MA).

2.2. Methods and characterization

2.2.1. Membrane casting

Casting solutions were prepared by dissolving the polymer resins and drug in solvent or solvent–nonsolvent mixtures, followed by sonication for 15 min and sitting for 30 min to remove air bubbles. Typical solutions consisted of 20–35 wt% PDLLA and PLGA, 10–12% PCL or 5–6% PLLA, 1–10 wt% naproxen, 60–80 wt% solvent, and 0–25 wt% nonsolvent. Solutions were film-cast on glass plates using a bar applicator with gap size of 500 μm. The membrane was then formed by dry and wet-cast phase inversion methods. In the former case, evaporation of solvent and nonsolvent was carried out under either free or forced convection conditions in a 35–45% relative humidity (RH) lab environment. Forced convection was carried out under a fume hood with an air velocity of 90 cm/s. Membranes formed under vapor-induced phase separation (VIPS) were dry-cast under 75% or 95% RH in an ETS Model 5500-8000 polycarbonate humidity-controlled chamber (Electro-tech system, Inc., Glenside, PA). For wet casting, the membrane was formed by evaporation of the casting solution on the plate for 1 min and then quenching into a 2-L nonsolvent bath. The membrane was solidified for 1–4 h prior to drying. All formed films were dried in a fume hood overnight, followed by a vacuum oven for an additional 3 days at room temperature. The resulting membrane thicknesses were in the range of 30–70 μm. Drug loads (DLs), defined as the weight percent of the drug in the dry naproxen/polymer membrane were between 0% and 40%. The upper limit on the DL was set by the solubility of the naproxen in the organic solvents. Several samples were also stored at room temperature with desiccant for periods up to 2 months in order to test for drug stability.

2.2.2. Membrane morphologies

Membrane morphologies and drug distribution in the polymer matrix were examined using a Hitachi S-4300 scanning electron microscope (SEM) under an accelerating voltage of 2 kV. Films were fractured in liquid nitrogen and mounted on a metal stub with a double-sided adhesive tape. The cross-section and surface of the membrane were sputter-coated with Au/Pd prior to SEM analysis.

2.2.3. Drug release profiles

In vitro drug release experiments were conducted using a Hanson Research SR8-Plus dissolution test station configured as USP apparatus 5 (paddle-over-disk). 3 cm × 3 cm films were inserted into USP 5 disks (Pharma Alliance) and placed in vessels containing 900 mL sodium phosphate buffer (50 mM, pH 7.4) equilibrated at 37 °C. The agitation speed was 50 rpm. Sample solutions were taken into HPLC vials at various times with 1 mL pipettes and were kept at 5 °C for concentration analysis. Analyses were made using a Waters 2690D high performance liquid chromatography (HPLC) system with a reversed phase column, Waters Symmetry Shield RP8 (4.6 mm × 50 mm, 5 μm), and UV detection at 229 nm. The mobile phase consisted of acetonitrile and 0.1% *o*-phosphoric acid (50:50, v/v). Naproxen concentrations were determined from calibration curves of standard with naproxen concentration of 38.03 μg/mL. A minimum of two replications were run for each experiment and the results are presented as averages. Relative standard deviations were in the range of 1–3%.

2.2.4. Polymer molecular weight degradation profiles

Degradation kinetics of the polymers were studied using a Waters 1515 gel permeation chromatography (GPC) system fitted with a Waters Styragel guard, a HR 1, and a HR 4 column connected in series. Both columns and the refractive index (RI) detector were equilibrated at 40 °C and chloroform was used as the mobile phase. Molecular weights of each sample were determined from a calibration curve of polystyrene standards (M_w ranging from 1680 to 560,000) and analysis was carried out using the software Breeze 3.20 with the method of GPC. A minimum of two replications were run for each experiment and the results were presented as averages.

2.2.5. Thermal properties

Thermal properties of the membrane/drug system, including drug melting temperature (T_m), heat of fusion (ΔH), and membrane glass transition temperature (T_g), were measured using a TA instruments 2920 differential scanning calorimeter (DSC). Samples of 5–20 mg were cut from cast films, sealed in aluminum pans, and heated from 25 to 250 °C at a rate of 10 °C/min. After a rapid quench to −10 °C, samples were reheated to 250 °C at the same heating rate. The endothermic melting peak for naproxen was recorded from the 1st heating cycle, and the glass transition temperature of the polymer was taken as the inflection point in the heat capacity increment during the second heating cycle. The degree of crystallinity of naproxen was calculated as follows:

$$\text{Crystallinity} = \frac{\Delta H_m}{\Delta H_0 \times \text{DL}} \times 100\% \quad (1)$$

where ΔH_m and ΔH_0 are the heat of fusion (J/g) for the naproxen/PBCA membrane and pure naproxen crystals (161.8 J/g), respectively. The percent of amorphous drug dissolved in the PBCA was estimated using Eq. (2), assuming 100% crystallinity for the precipitated drug crystals:

$$\%\text{Amorphous} = \frac{\text{DL}(1 - \text{Crystallinity})}{1 - \text{DL} \times \text{Crystallinity}} \times 100\% \quad (2)$$

All samples were run in duplicate. In order to determine naproxen stability in the cast films, DSC runs and drug release runs were made on the stored samples mentioned above. No noticeable changes in drug crystallinity or T_g occurred, nor were any significant changes observed in the release kinetics of the aged films compared to the freshly cast samples.

2.2.6. Cloud point curves (binodal curves)

Cloud point measurements were made on polymer/solvent/naproxen solutions for several of the systems. Stirred solutions were titrated with nonsolvent water at 25 °C until permanent visual turbidity was achieved. The final solution concentrations were plotted as volume % of each component on a polymer/solvent/water ternary phase diagram.

3. Results

3.1. Drug–polymer compatibility and drug plasticizing effects

As shown in our earlier studies, (Ma and McHugh, 2007; Ma, 2008), drug–polymer compatibility can be estimated by comparing solubility parameters for the systems, calculated by group contribution methods, and the associated heats of mixing. However, a more direct measure of the solubility characteristics of the as-cast films is thermal analysis. In this case, the % solubility, SA, of the naproxen in the polymer at the melting point (T_m) is estimated from the relation between DL and drug–polymer heats of fusion (ΔH) (Li et al., 2002; Ma and McHugh, 2007):

$$\text{DL} = S_A + \frac{100 - S_A}{\Delta H^0_{SC}} \Delta H^0(\text{DL}) = S_A + k\Delta H^0(\text{DL}) \quad (3)$$

ΔH^0(DL) and ΔH^0_{SC} are the heat of fusion of the drug in the film and pure form, respectively, and k is the slope. Fig. 1 shows DSC solubility plots for the PLA systems. From these data, the extrapolated solubilities of naproxen in the PLGA, PDLLA, and PLLA as-cast

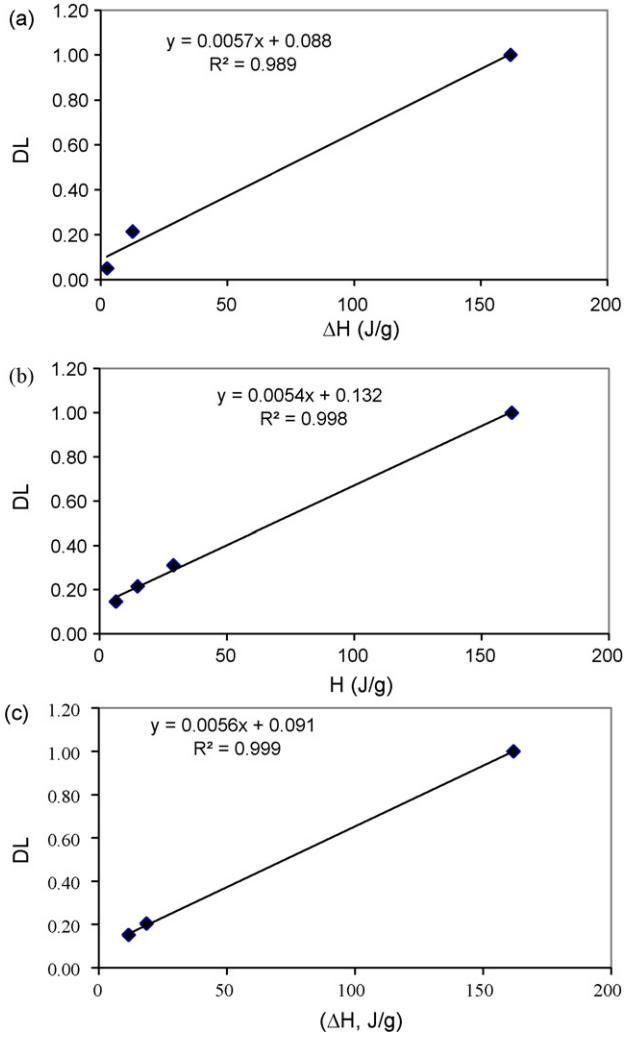

Fig. 1. Naproxen solubility plots for (a) PLGA film, (b) PDLLA film and (c) PLLA film.

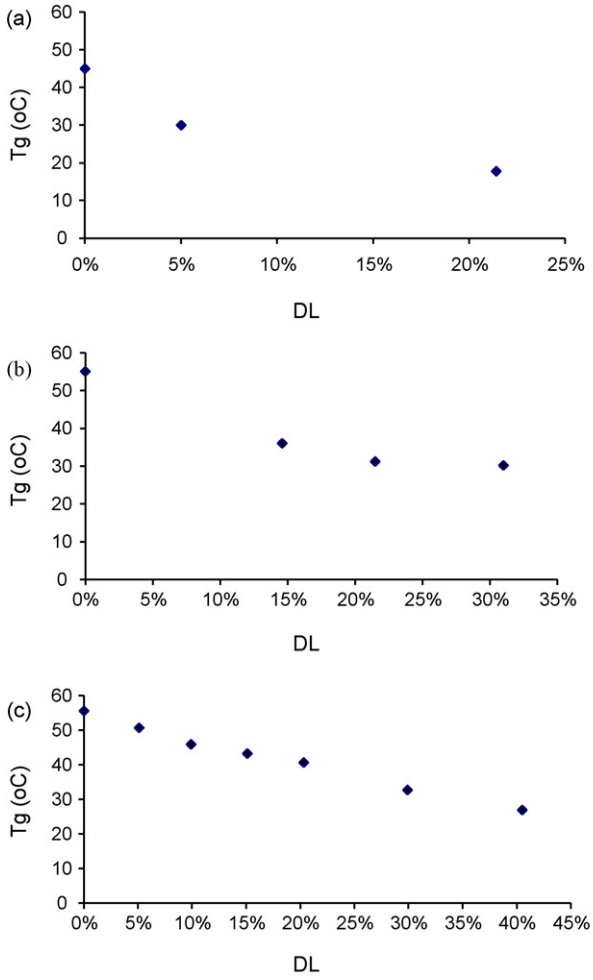

Fig. 2. Effect of DL on the glass transition temperature (T_g) for (a) PLGA film, (b) PDLLA film and (c) PLLA film.

films are 9%, 13%, and 9%, respectively. Overall solubilities for the three systems are lower than in CA (22%), consistent also with the theoretical estimation (Ma and McHugh, 2007; Ma, 2008).

Fig. 2 shows T_g data obtained from the second DSC scans for the polylactide samples with 0–40% DL. All samples exhibited a single T_g between that of the polymer and that of the naproxen, $T_g = -24\,^{\circ}C$ (Nair et al., 2001), indicating complete miscibility of the polymer–drug in this concentration range. The data for the PLGA membranes show that, as the DL increases from 0% to 22%, the polymer–drug T_g decreases from 45 °C for the pure PLGA to about 18 °C. Similar T_g decreases are observed for PDLLA and PLLA films; however, the plasticizing effects in all three polymers are not as dramatic as that exhibited by the CA–naproxen systems (Ma and McHugh, 2007).

3.2. Polymer–solvent–nonsolvent phase diagrams and the role of naproxen on the structure formation of quenched films

PLGA and PDLLA are amorphous polymers with good solubility in acetone. Experimentally determined cloud point data and associated binodal curves for the PLGA–acetone–water and PDLLA–acetone–water systems (figures not shown) showed the binodal curves for the two are essentially the same. However, the binodals were much closer to the polymer–solvent line compared with the CA–acetone–water system, indicating less compatibility with the acetone–water system. Based on the cloud point data, the starting nonsolvent compositions in the casting solutions for PLGA and PDLLA systems were generally kept below 8–10% in order to maintain homogeneity. By contrast, the PLLA, a semi-crystalline polymer (T_m ~175–185 °C), is soluble in only a few organic solvents, such as chloroform, dioxane or dichloromethane. Ternary phase diagrams have been reported for two such cases: PLLA–dichloromethane–ethanol (Liu et al., 2004) and PLLA–chloroform–methanol (van de Witte et al., 1996a). Depending on the starting compositions and mass transfer path, phase inversion for these systems can occur either by liquid–liquid (l–l) demixing followed by locking-in due to crystallization, or by solid–liquid (s–l) demixing. Generally, l–l phase separation results in a porous two-phase structure, while s–l demixing leads to a more uniformly dense structure (van de Witte et al., 1996b).

Figs. 3i–iv and 4a–f show the as-formed morphologies for naproxen–PLGA–acetone and naproxen–PDLLA–acetone membranes, respectively, for DLs below and above the solubility limit. For DL below or close to the solubility limit, membrane structures in both systems are uniformly dense with no observable drug particles, reflecting the fact that the naproxen is fully dissolved in the as-cast polymer film. (The small particles in Figs. 3ii and 4a–c are ice which condenses from the air when the film is fractured under liquid nitrogen prior to SEM irradiation.) By contrast, for DL's above the solubility limit, needle-like particles of naproxen are clearly visible, dispersed throughout the membrane matrix. Similar to what was observed earlier with the CA films (Ma and McHugh,

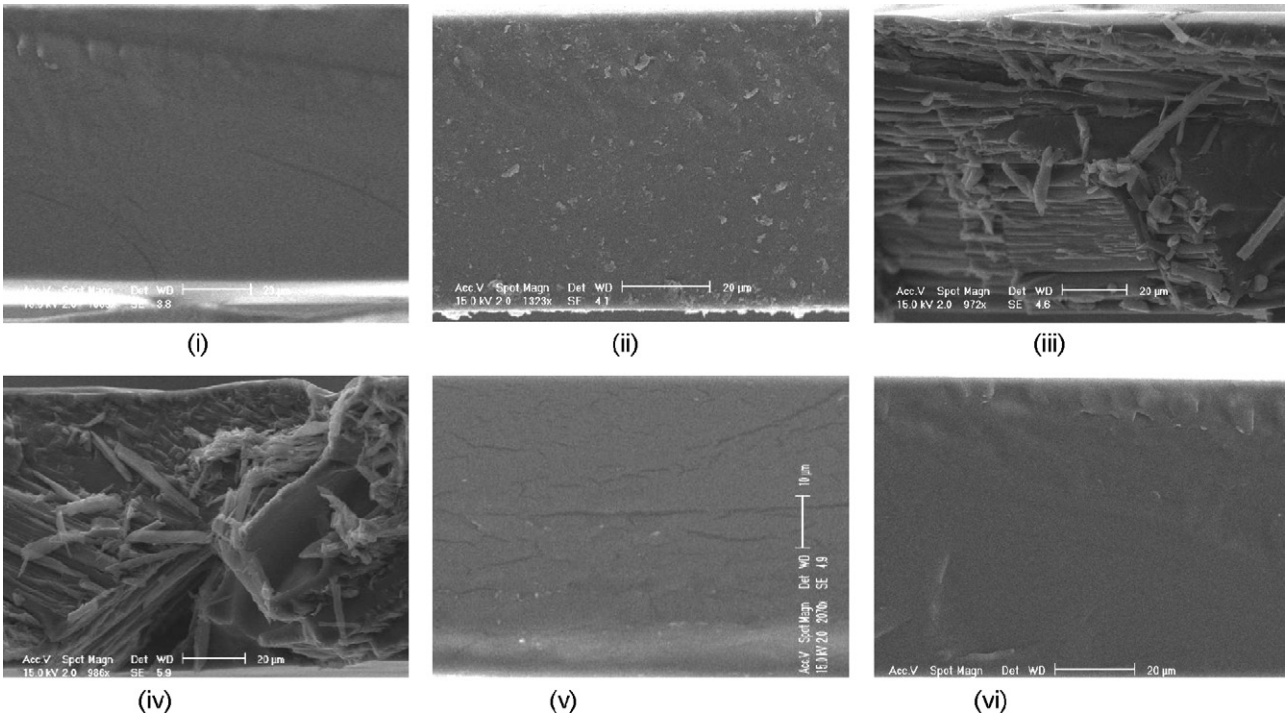

Fig. 3. Morphologies of PLGA/acetone/naproxen membranes with different DL. (The top surface represents the air–solution interface, i-0% DL, ii-5% DL, iii-21% DL, iv-36% DL, v-21% DL and 5% water, vi-23% DL and 5% water, [PLGA] = 33 wt%, no water is present in the casting solutions of i–iv.)

2007), the lack of phase inversion and occurrence of uniformly dense films indicate that naproxen does not function as a phase-separating agent (i.e. nonsolvent) in either system. On the other hand, PLGA–acetone–naproxen films cast from initially homogeneous solutions containing 5% nonsolvent water turn opaque after a few minutes, indicating formation of a two-phase structure. However, as evaporation proceeds, films revert back to a completely clear state and at the end of the solidification process exhibit a uniformly dense structure as shown in Fig. 3v and vi. This is similar to what was observed in an earlier study of PLGA cast films (van de Witte et al., 1996b) and with CA–naproxen (Ma and McHugh, 2007). In the present case, locking-in of the two-phase structure is inhibited by the intrinsically low T_g of PLGA, while in the latter case (CA–naproxen), the plasticizing effect of the drug, lowers the polymer T_g, causing the collapse of the two-phase structure and reversion to a homogeneous state.

3.3. Relation of film morphology to the drug release kinetics

The impact of membrane morphology on the drug release kinetics of the PLGA and PDLLA systems is illustrated in Figs. 5 and 6. Since, 5% DL PLGA films cast with either 0% or 5% water have a dense structure; their release profiles are very similar. Likewise, the 5% and 10% DL PDLLA films exhibit similar release profiles, with the expected higher release rate with increased DL. By contrast, the higher drug load films in both cases exhibit a burst release pattern,

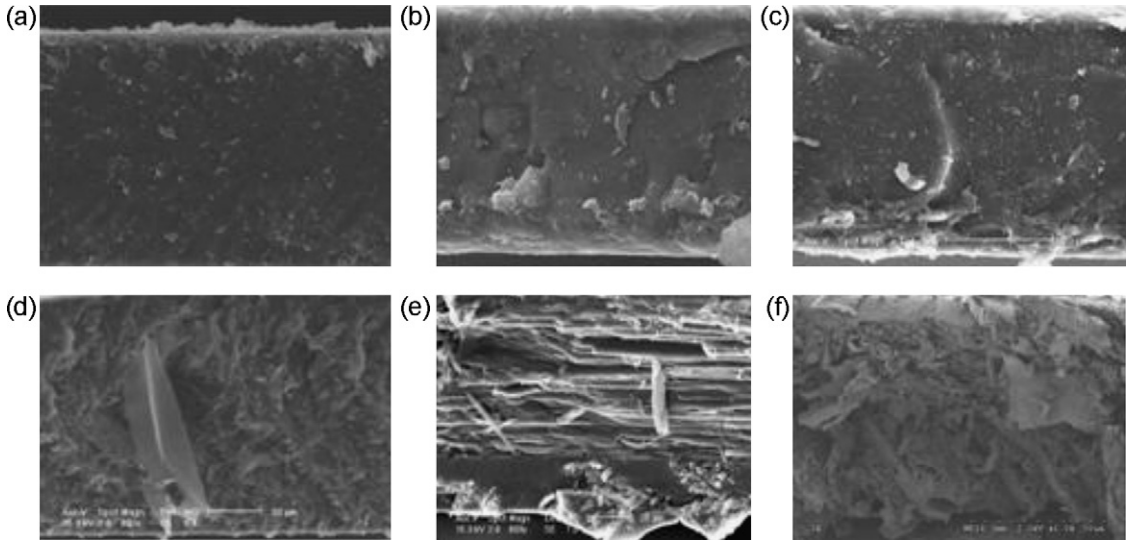

Fig. 4. Morphologies of PDLLA/acetone/naproxen membranes with different DL. (The top surface represents the air–solution interface, a-0% DL, b-5% DL, c-10% DL, d-15% DL, e-22% DL, f-37% DL, [PDLLA] = 30 wt%.)

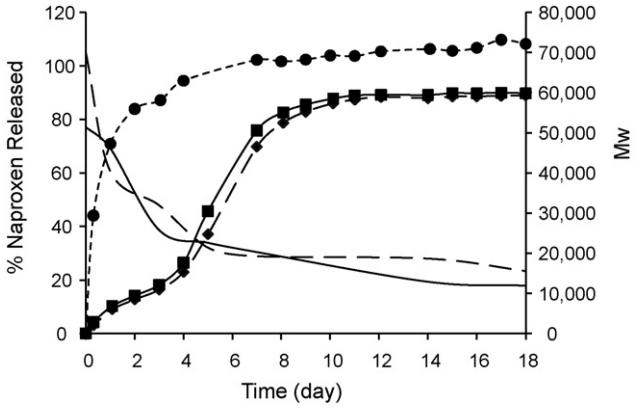

Fig. 5. Naproxen release profiles overlaid with PLGA degradation kinetics from naproxen/PLGA/acetone/water membranes with different DL. Symbols: (●) 21% DL, 0% water; (■) 5% DL, 5% water; (♦) 5% DL, 0% water. Dashed line: M_w (5% DL, 0% water); solid line M_w (5% DL, 5% water).

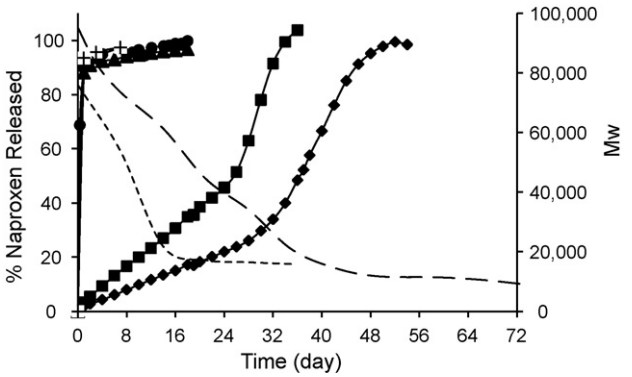

Fig. 6. Naproxen release profiles overlaid with PDLLA degradation kinetics from naproxen/PDLLA/acetone membranes with different DL. Symbols: (♦) 5% DL; (■) 10% DL; (▲) 15% DL; (●) 22% DL; (+) 37% DL. Heavy dashed line: M_w (5% DL); light dashed line: M_w (10% DL).

due to the fast dissolution of the long needle-like drug particles (Figs. 3iii, iv and 4e, f).

In both cases, the release curves for the low DL films exhibit a two-stage pattern. The initial release stage for the PLGA is a more-or-less diffusion-controlled parabolic profile (Fig. 5), while the PDLLA first stage is zero-order release (Fig. 6). In this stage, significant polymer degradation also occurs with both systems, as shown by the sharp decrease in the M_w. However, in both systems the film mass was found to be constant, indicating that significant polymer erosion has not started. Hence, depending on the interplay of polymer degradation and drug diffusion through the polymer matrix, the release can exhibit either a diffusion-controlled profile as shown in Fig. 5 or a degradation-controlled near zero-order release profile as seen for the PDLLA system (Fig. 6). The data in Fig. 5 suggest that, prior to erosion; increases in the release rate are due primarily to the increased diffusivity resulting from the decrease in polymer molecular weight, which also apparently occurs at more-or-less constant morphology. Once the M_w decreases to a certain level (about 4 days) the increased solubility of the oligomers in the dissolution medium, reflected in a measurable mass loss, leads to the onset of an erosion-controlled release process which shows as a zero-order release profile. For the PDLLA, the zero-order release kinetics during the first stage is due to the continuous increase of

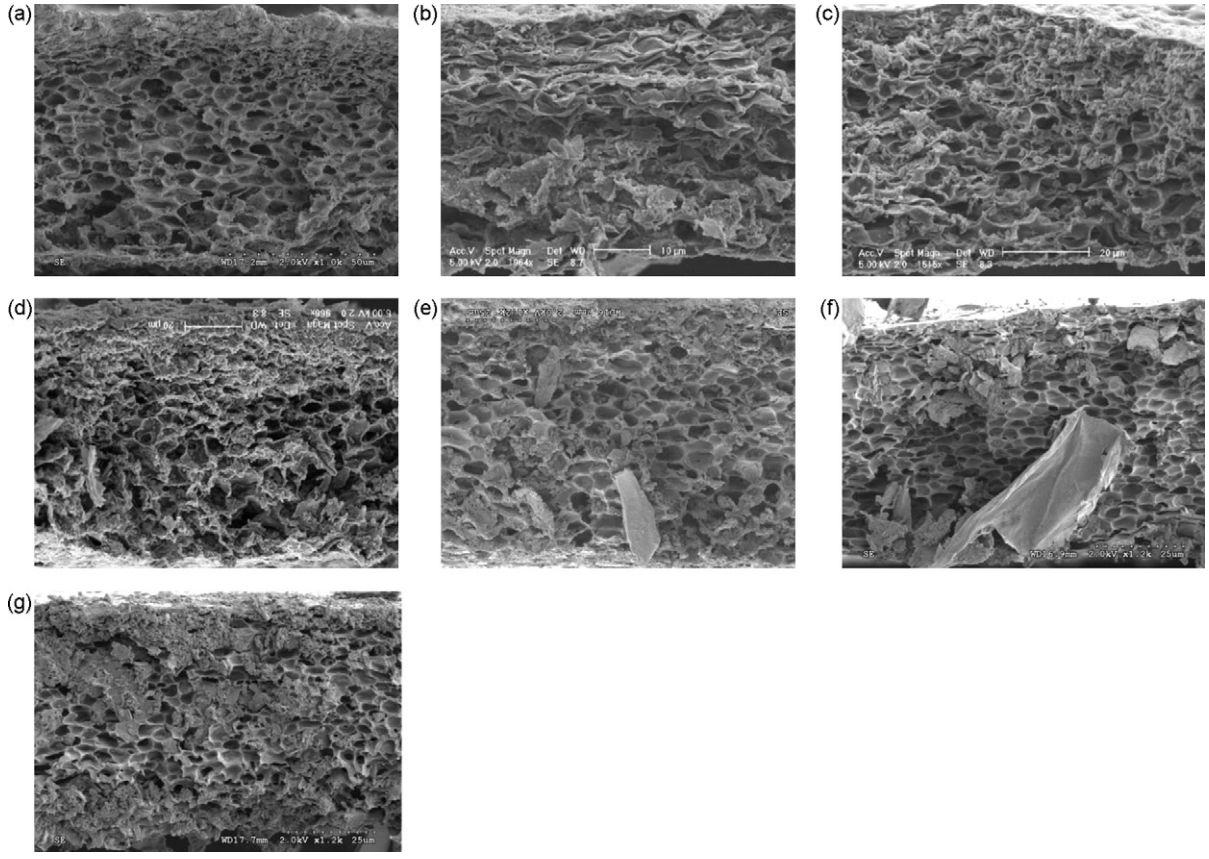

Fig. 7. Morphologies of PLLA/dichloromethane/naproxen/ethanol membranes cast from solutions containing 25% ethanol. (The top surface represents the air–solution interface, a-0% DL, b-5% DL, c-10% DL, d-15% DL, e-20% DL, f-30% DL, g-41% DL, [PLLA] = 5 wt%.)

drug diffusivity in the polymer matrix and the zero-order profile at the second stage is likely due to an erosion-controlled mechanism. These observations are put on a more quantitative basis in Section 3.10.

The morphologies of the PLLA–dichloromethane–naproxen films with DLs beyond the solubility limit (9%) (i.e. from 20% to 40%) were found to be similar to those of the PLGA and PDLLA systems above their solubility limits (i.e. dense films with precipitated needle-like drug particles — figures not shown). Accordingly, the release profiles of these two films also exhibited a burst release pattern, followed by shut-down (figures not shown). Apparently the burst effect cannot be avoided for these single-phase dense films when the DL is above the solubility limit.

3.4. Effect of DL on membrane morphology and drug release

In order to investigate the role of phase inversion and determine whether porous structures could be locked-in at high DL, a series of films having various DLs were cast from solutions containing nonsolvent. Similar to the PLGA films cast with 5% water, (see Fig. 3v and vi), all of the high DL PDLLA films exhibited uniformly dense structures with precipitated drug particles. By contrast, CA films cast under similar conditions exhibited a two-phase honeycomb structure (Ma and McHugh, 2007). Apparently, locking-in of the porous two-phase structure is inhibited in the PDLLA films due to the low glass transition temperature of the polymer, similar to that found with the PLGA films discussed in the previous section. Likewise, a two-stage, near zero-order release profile occurs with the 5% DL membrane, while the drug release profiles for the high DL films (DL > 10%) exhibit a burst release (figure not shown). This is consistent with and further supports the previous findings indicating that membrane morphologies and drug distributions within them have a profound effect on drug release kinetics.

Fig. 7 shows the morphologies of PLLA membranes cast from PLLA–dichloromethane–ethanol solutions containing 25% ethanol. The polymer concentration was maintained at 5% to ensure that the mass transfer path during quenching proceeds through the l–l demixing line, in which phase inversion can be locked-in by PLLA crystallization. As expected, all the films across the DL range exhibit a phase-separated structure with a dense skin and a uniform, honeycomb structure underneath. The absence of particles for low drug loads (<10%), reflects the fact the naproxen is dissolved in the PLLA-rich phase. For DL near and beyond the solubility limit, e.g. 10% DL, precipitated drug particles can be seen in the structure. However, in contrast to the CA membranes (Ma and McHugh, 2007), in which the precipitated drug particles were embedded into the honeycomb pores, the drug particles in the PLLA membranes precipitated as either large needles or plates outside the pores (Fig. 7e and f), or as clusters (Fig. 7g). This different drug distribution is likely due to the rejection of the drug from the crystalline regions of the PLLA, which inhibits their incorporation into the pores or walls. As a result, the release profile exhibits a burst behavior as seen in Fig. 8. The drug release profile for the 5% DL film exhibits a single-stage, more-or-less diffusion-controlled release pattern. In this case, due to the relatively slower degradation rate, significant polymer erosion did not occur on the time scale of the release, leading to the absence of a second stage erosion-controlled release. Quantitative modeling of these data is also given in Section 3.10.

3.5. Effect of nonsolvent content on membrane morphology and drug release

To investigate the effect of nonsolvent content on the morphological transitions and drug release characteristics of the PLLA membranes, a series of experiments was carried out with films cast from solutions having a fixed DL of 40% and ethanol contents from

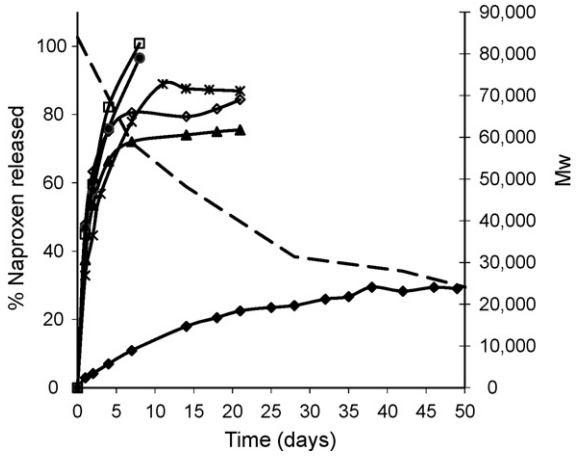

Fig. 8. Naproxen release profiles overlaid with PLLA degradation kinetics from naproxen/PLLA/dichloromethane/ethanol membranes cast from solutions containing 25% ethanol and indicated DLs. Symbols: (♦) 5% DL; (▲) 10% DL; (◊) 15% DL; (*) 20% DL; (●) 30% DL; (□) 40%. Dashed line: M_w, 10% DL.

0% to 25%. Fig. 9 shows the membrane morphologies. For ethanol contents less than 10%, a more-or-less dense, single-phase film with long, needle-like or plate-like naproxen crystals is obtained, indicating that no phase inversion occurs. This clearly suggests that, at low ethanol contents, the mass transfer path crosses the s–l demixing line, leading to polymer crystallization. With increasing ethanol content (20%) the morphology transforms to the honeycomb structure, indicating that the mass transfer path proceeds to the l–l demixing line with subsequent locking-in of the phase-inverted structure by crystallization. The structural transformation continues with increasing ethanol content, eventually reaching the well-defined honeycomb morphology with a dense polymer-rich skin at the air–solution interface (Fig. 9e). Most of the precipitated drug particles are dispersed as plates or clusters outside of the pores with very few embedded in the pores. This pattern of increasing two-phase structure formation with increasing nonsolvent content is also consistent with the CA films (Ma and McHugh, 2007). However, the formation mechanisms are different, i.e. l–l demixing followed by locking-in due to glassification in the CA systems, and l–l demixing followed by locking-in due to crystallization in the PLLA systems.

Naproxen release rates (figure not shown) exhibit bursting for all the membranes. The dense films cast with 0–10% ethanol content exhibited complete drug release within 1 day while, in contrast, release from the film cast with 25% ethanol is much slower due to the partial sequestering of small drug crystals in the pores (Fig. 9e).

Similar to PLLA, PCL is a semi-crystalline biodegradable polymer; however, it has a much lower T_g (−65 °C). At low water contents (5% and 7.5%), the system undergoes s–l demixing, resulting in a more-or-less dense single-phase structure with long precipitated drug particles (figure not shown). Consequently, the drug release was found to exhibit a burst of 100% in a 24-h period (figure not shown).

3.6. Effect of polymer concentration on membrane morphology and drug release

To explore the effect of polymer concentration, PLLA membranes with 20% DL were cast with 25% ethanol and four concentrations of PLLA — 5%, 10%, 15%, and 20%. Fig. 10 shows the as-formed film morphologies. The 5% PLLA membrane shows a typical two-phase structure with a thin dense skin and a honeycomb structure underneath. Other than some large pieces, most of

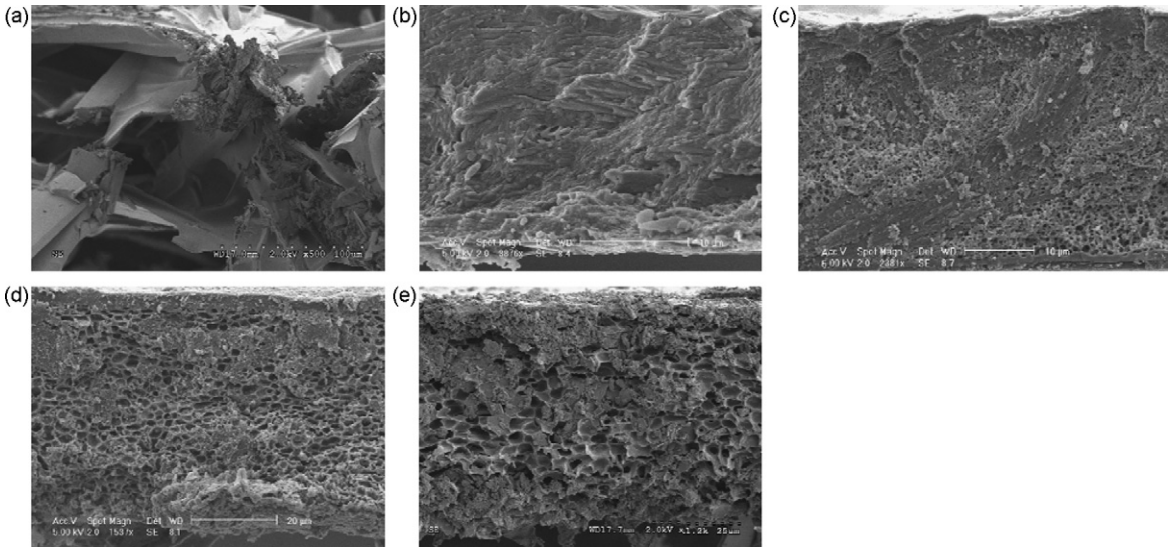

Fig. 9. Morphologies of naproxen/PLLA/dichloromethane membranes with 40% DL cast from solutions containing various ethanol concentrations. (The top surface represents the air–solution interface, a-0% ethanol, b-5% ethanol, c-10% ethanol, d-20% ethanol, e-25% ethanol, [PLLA] = 5 wt%.)

the precipitated drug particles appear as clusters embedded in the pores. With increasing polymer concentration, the skin becomes thicker and the two-phase structure eventually collapses to form a single-phase dense film at 20% PLLA concentration (Fig. 10d). As discussed in Sections 3.3 and 3.4, the morphological transition is likely due to the mass transfer path being diverted from the l–l demixing line (5%, 10% and 15% [PLLA]) to the s–l binodal curve (20% [PLLA]), which induces PLLA crystallization and formation of a dense film. The drug release curves exhibited a monotonic increase with PLLA concentration starting from a more-or-less diffusion-type control at 5% PLLA and followed by a bursting profile at the higher PLLA concentrations (10–20% PLLA) (figure not shown). The reduced burst release at the lower PLLA concentration likely reflects incorporation of the drug particles into the pores; however, this apparently occurs only for the lowest drug concentration (5%).

3.7. *Effect of casting conditions on membrane morphologies and drug release*

The effect of casting methods and conditions on morphologies and drug release rates for PDLLA films was studied by comparing membranes cast under free convection, forced convection, wet-cast (quench), or vapor-induced phase separation conditions. Fig. 11 shows the as-formed membrane structures for the 5% DL film. The dry-cast films exhibit a single-phase dense structure (Fig. 11i and ii), whether formed under free or forced convection conditions. This

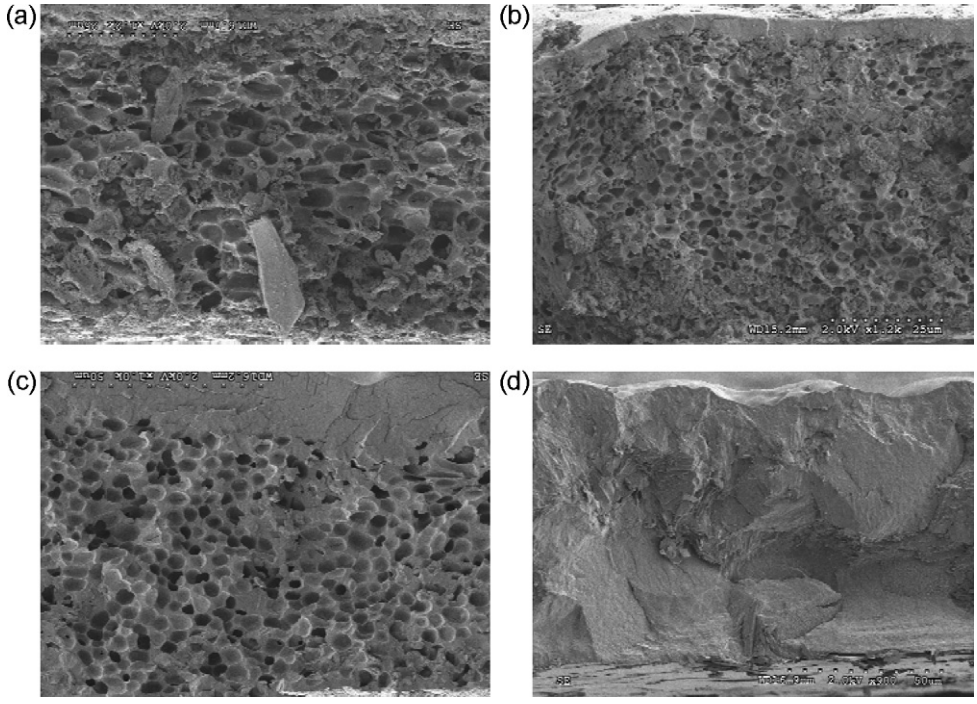

Fig. 10. Morphologies of PLLA/dichloromethane/naproxen/ethanol membranes with 20% DL cast from solutions containing 25% ethanol. (The top surface represents the air–solution interface, a-5% [PLLA], b-10% [PLLA], c-15% [PLLA], d-20% [PLLA].)

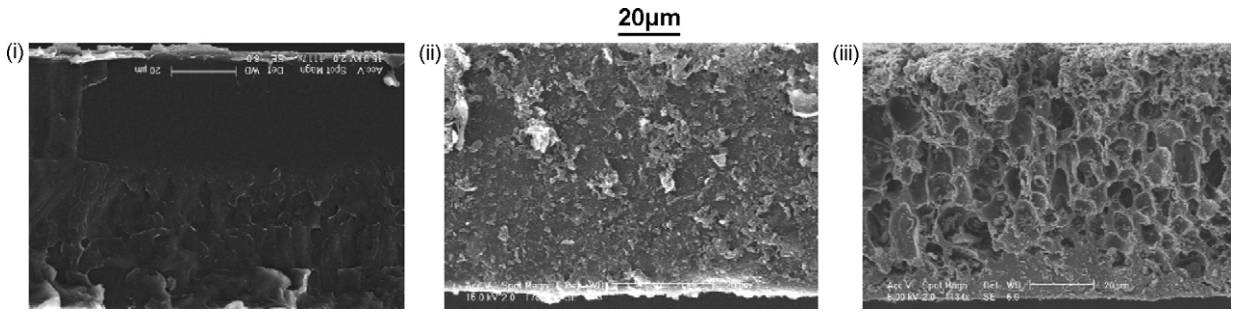

Fig. 11. Morphologies of PDLLA/acetone/naproxen membranes with 5% DL cast under different conditions with 8% water. (The top surface is the air–solution interface, i-free convection, ii-forced convection, iii-wet-cast.)

likely reflects the low T_g of PDLLA which inhibits locking-in of the phase-separated structure. By contrast, the phase-inverted porous structure can be locked-in by wet casting, as seen in Fig. 11iii. This is likely due to a much more rapid solvent–nonsolvent exchange in the bath that reduces the solvent plasticizing effect and keeps the polymer T_g high enough to allow locking-in of the phase-inverted structure. Release rates for the free and forced convection films were found to be similar and slightly slower than that of the wet-cast film (figure not shown). The morphologies of 37% DL PDLLA films dry-cast under free conditions films, exhibited a dense single-phase structure with precipitated drug particles, while the wet-cast film exhibited a porous morphology containing macrovoids from which long needle-like drug crystals appeared to have been extruded (figures not shown). In both cases, the release curves showed a burst with 100% released in 1 day (figures not shown).

Morphologies of the 0% DL PDLLA films cast under 75% and 95% RH via the VIPS process all exhibited a dense, single-phase structure, regardless of the humidity level (figures not shown). The films became opaque as water began to precipitate from the vapor, indicating the initiation of phase inversion. However, the films became completely clear after removal from the humidity chamber and drying under ambient conditions. This phenomenon again reflects the inability of the phase-inverted structure to lock in due to the low polymer T_g.

3.8. Effect of polymer blending on membrane morphology and drug release

Results described in the previous section indicate that the phase-inverted structure of PLLA membranes can be locked-in by polymer crystallization. However, the precipitated drug particles in the high DL films are excluded from the honeycomb pores due to repulsion from the polymer crystalline regions, thereby leading to a burst release. By contrast, naproxen has good compatibility and can be molecularly dissolved in amorphous PDLLA. However, the phase-separated structure for that system cannot be locked-in due to the low T_g of the polymer. To further investigate this aspect, a PDLLA–PLLA blend system was studied. The objective was to deter-

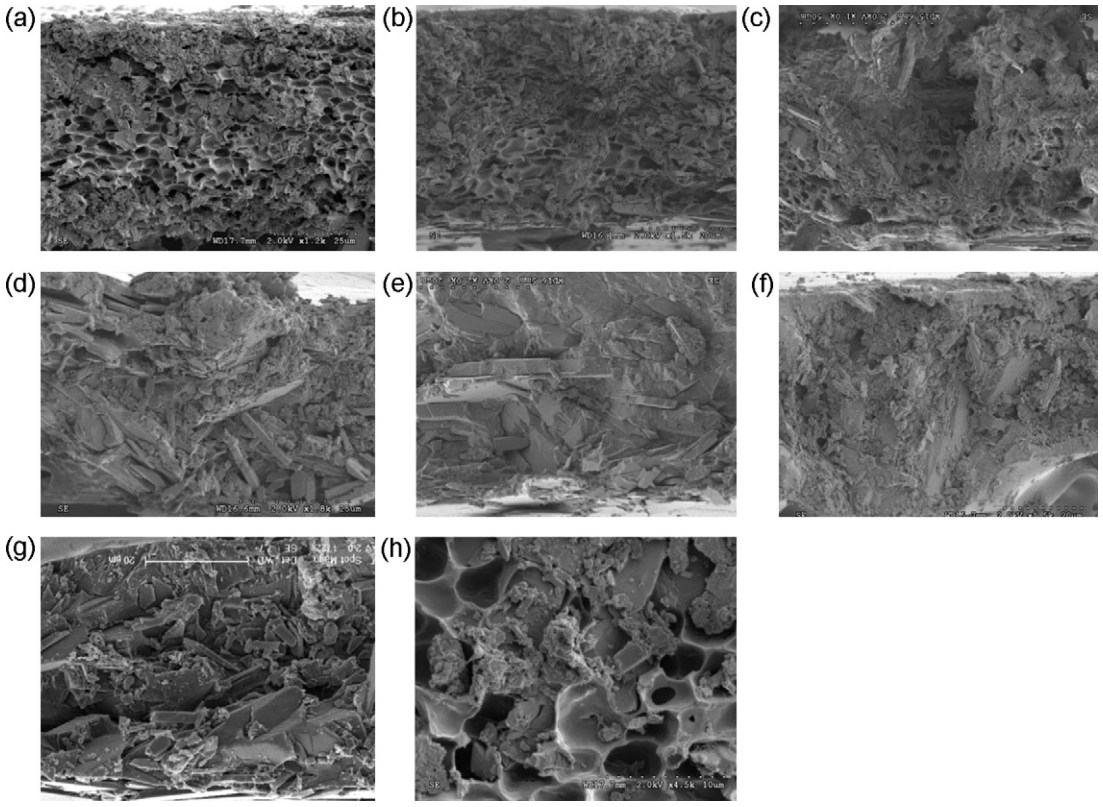

Fig. 12. Morphologies of PLLA–PDLLA/dichloromethane/naproxen membranes with 40% DL and cast from solutions containing 25% ethanol. (The top surface represents the air–solution interface, a-100% PLLA, b-90% PLLA, c-70% PLLA, d-50% PLLA, e-30% PLLA, f-10% PLLA, g-0% PLLA, h-100% PLLA magnified porous region, [PDLLA + PLLA] = 5 wt%.)

mine whether the lock-in feature of the crystalline PLLA and good compatibility feature of PDLLA film could be combined to produce high drug load-nonbursting films.

Fig. 12 shows as-formed membranes for PLLA–PDLLA blends with 40% DL. The 100% PLLA film exhibits a classic honeycomb structure (Fig. 12a) with some embedded drug particles (Fig. 12h). As the PLLA content decreases below 70%, the membrane changes from a two-phase porous structure to a single phase, dense structure with large pieces of precipitated drug particles dispersed within the polymer matrix (Fig. 12d–g). This indicates that the low T_g of the PDLLA dominates the morphology formation in these films, leading to the collapse of the phase-inverted structure.

The more-or-less dense films with PLLA content ≤70% exhibited sharp burst release profiles (100% release in 1 day) with significantly reduced bursting for the 100% PLLA film (100% release in 7 days) (figures not shown). The latter reduction in release rate is likely due to the incorporation of the small drug particles in the honeycomb pores (Fig. 12h).

3.9. Effect of solvent properties on membrane morphologies and drug release

Since solvent properties could affect the shape or location of the binodal curve on the ternary phase diagram, their effects on PDLLA and PLLA films were evaluated. The morphologies for PLLA films cast from solutions containing chloroform and methanol as a solvent and nonsolvent and 10% or 45% DL all exhibited a uniformly dense structure when cast by free or forced convection with 20% methanol in the casting solution (figures not shown). The apparent lack of phase inversion can be explained with the PLLA–chloroform–methanol ternary phase diagram illustrated in van de Witte et al. (1996b). Since the PLLA content is kept at 10% and the methanol content is 20%, the mass transfer path likely crosses the s–l line, so that solid–liquid demixing occurs and polymer crystallization leads to a single-phase, dense film. Drug release profiles for these films (figures not shown) showed a 100% burst release for the 45% DL films owing to the fast dissolution of the precipitated drug particles with connections to the membrane surface. The 10% DL film showed a small burst of 15% with a sustained release profile (figure not shown), which was significantly slower than the same DL porous film-cast with dichloromethane–ethanol (see Fig. 9). The latter shows a 35% burst followed by a fast release pattern. This may reflect the lower drug diffusivity in the dense membrane structure as opposed to that in the porous membrane structure.

PDLLA membranes were also cast with dichloromethane–ethanol and chloroform–methanol. The 20% and 35% DL films exhibited a dense structure with long precipitated drug particles (figures not shown). Similar to the acetone–water system, the single-phase structure likely resulted from the inhibition of locking-in of the phase-inverted structure due to the low T_g of the PDLLA films. Consequently, both films showed an 80% burst release due to the fast dissolution of the drug particles (figures not shown).

3.10. Quantification of the drug release kinetics

PLGA, PDLLA, and PLLA are generally believed to undergo bulk erosion, with erosion progressing homogeneously throughout the polymer matrix (Alexis, 2005). Investigation of membrane morphologies for 10% DL PLLA films at different dissolution times showed that the initially dense film changes to a leafy structure with scattered pores throughout after 7 days in the dissolution bath, while also exhibiting only slight polymer degradation (Ma, 2008). After 72 days, the number of pores increased dramatically indicating a larger extent of degradation. Most of the pores were close to the membrane–dissolution medium surface region due to the very low diffusion rate at the membrane–USP 5 disk surface. The distribution of the pores would be expected to be uniform throughout the membrane matrix if both sides of the membrane were in touch with the dissolution medium directly. These results confirm that PLLA undergoes bulk degradation in the *in vitro* dissolution medium. It is interesting to note that even with naproxen, a weak acid, auto-acceleration of the degradation, as reported in literature (Li et al., 1990a,b,c), that would have led to faster erosion in the middle than at the surface of membrane, was not observed.

As discussed in Section 3.3, the release kinetics can be quantified in terms of a two-stage release mechanism. During the first stage, polymer degradation, showing as a sharp molecular weight decrease, occurs; thus the dissolution is by a combination of polymer degradation and drug diffusion in the membrane matrix. Since as indicated, the total system mass remains more-or-less constant in this stage, release occurs at more-or-less constant morphology. In the second stage, the molecular weight drops to the level at which oligomers are soluble in the medium, thus significant polymer erosion results as a mass loss. In this stage, the drug release is modeled as an erosion-controlled, zero-order mechanism.

During the first stage, the polymer degradation, i.e. molecular weight reduction, can be fit by the following inverse, second-order polynomial relationship.

$$\frac{M_w}{M_{w0}} = \frac{1}{1 + at + bt^2} \tag{4}$$

where M_{w0} and M_w are the polymer molecular weights at the beginning of and during the dissolution, respectively, t is the dissolution time, the coefficients a and b are fit to the molecular weight data. Drug transport through the rubbery polymer matrix can be quantified in terms of the Stokes–Einstein equation (Bird et al., 2002) for a viscous melt,

$$D = \frac{k_B T}{6\pi\eta r} \tag{5}$$

where D is the drug diffusivity, k_B is Boltzmann's constant, T is the absolute temperature, η is the viscosity of the polymer matrix, and r is the equivalent molecular radius of the (assumed) spherical drug particle. Since for molecular weights below the entanglement value, the viscosity varies linearly with M_w (Kumar, 1980), combination of Eqs. (4) and (5), gives the following expression for the time dependence of the drug diffusion coefficient:

$$D = D_0(1 + at + bt^2) \tag{6}$$

where D_0 is the initial drug diffusivity. The diffusive release rate can be described using the standard modification of the Fickean diffusion equations with a time-dependent diffusivity (Crank, 1975).

$$\frac{M_t}{M_\infty} = 4\left(\frac{T}{\pi l^2}\right)^{1/2} \quad \text{for } 0 \le \frac{M_t}{M_\infty} \le 0.6 \tag{7}$$

$$\frac{M_t}{M_\infty} = 1 - \frac{8}{\pi^2}\exp\left(-\frac{\pi^2 T}{l^2}\right) \quad \text{for } 0.4 \le \frac{M_t}{M_\infty} \le 1.0 \tag{8}$$

where, the modified time, T is given by

$$T = \int_0^t D dt = D_0 \int_0^t (1 + at + bt^2) dt = D_0 t\left(1 + \frac{1}{2}at + \frac{1}{3}bt^2\right) \tag{9}$$

In these expressions, l is the membrane thickness, k is the release rate constant, and M_t/M_∞ is the fraction of drug released. D_0 can be calculated by fitting the experimental release data, and from this, the complete release profiles can be predicted using Eqs. (7) and (8).

In the second stage, drug release is mainly controlled by the polymer erosion. Expressing this as a zero-order release process gives:

$$\frac{M_t}{M_\infty} = k_d t \tag{10}$$

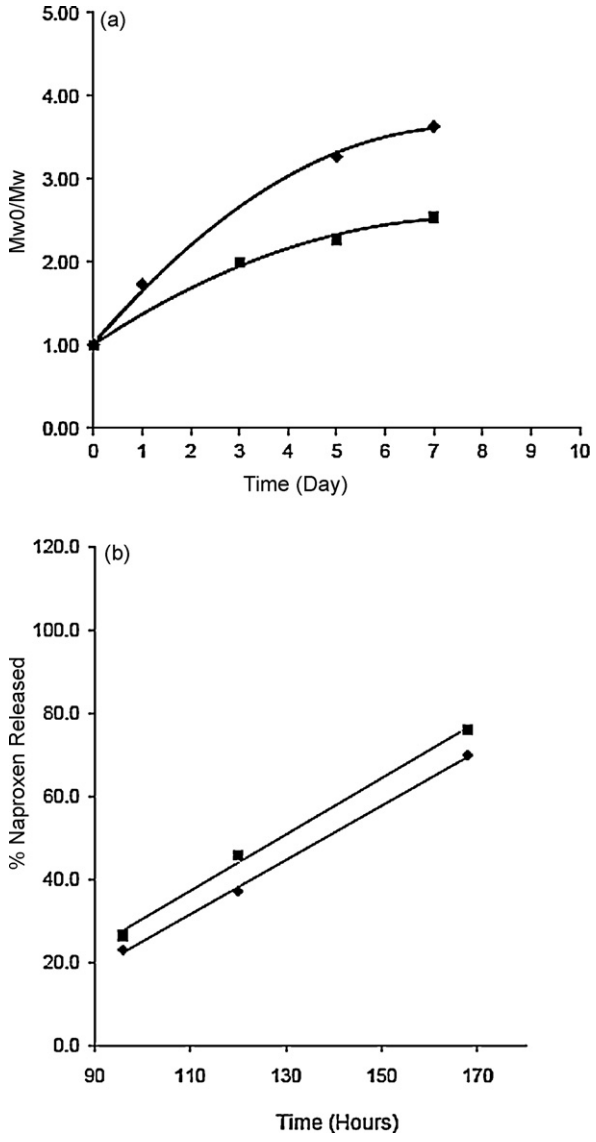

Fig. 13. Plots of model fit with experimental data for 5% DL PLGA–acetone films. (a — inverse polynomial curve fit for the polymer degradation profiles, b — linear plots of release fractions versus time at the second stage of release.) Symbols: (▲) 0% water; (■) 5% water.

The polymer erosion rate constant, k_d, is obtained from the release fraction versus time curve for the second stage of release.

3.10.1. PLGA membrane release

The release curves for the 5% DL PLGA films cast from 0% to 5% water solution, respectively, are illustrated in Fig. 13. The fit in Fig. 13a is for the first stage (0–4 days) degradation kinetics and Fig. 13b illustrates the zero-order fit for the second release stage (4–7 days). Table 1 summarizes the resulting parameters. The diffusivities and erosion rate constants are comparable for both systems, suggesting that the diffusion rate of the dissolved amorphous drug is similar for these two dense films with similar erosion rate. Fig. 14 shows the overall release profiles for the 5% DL films predicted by

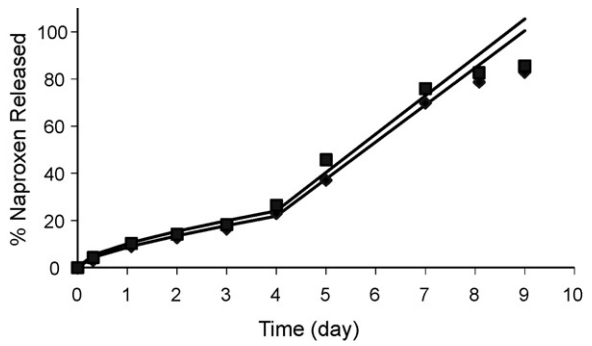

Fig. 14. Plots of model predications and experimental data for 5% DL PLGA–acetone films cast from solutions containing 0% or 5% water (symbols — experimental data, lines — model predictions). (▲) 5% Dl, 0% water; (■) 5% DL, 5% water.

Table 2
Drug release kinetics results for PDLLA–acetone membranes with 0% water in the casting solution.

Sample	a (day^{-1})	b (day^{-2})	R^2 (M_w)	D_0 (cm^2/s)	k_d (h^{-1})	R^2 (k_d)
5% DL	0.0248	0.0014	0.9955	5.32E-14	0.1705	0.9913
10% DL	0.1800	−0.0007	0.9933	1.20E-13	0.2597	0.9914

the two-stage models. The data are well fit in the first stage and most of the second stage, however, the plateau at the final stage is not.

3.10.2. PDLLA membrane release

The drug release profiles for 5% and 10% DL PDLLA films cast from 0% water solutions, were analyzed; however, due to the severe burst release profiles, the high DL films (DL > 10%) were not. Similar to the PLGA system, release profiles for the PDLLA membranes show a typical two-stage pattern with a longer polymer degradation stage (first stage) but fast erosion rate (second stage) (see Figs. 5 and 6). Fig. 15a and b show the inverse polynomial fit for the molecular weight data, and the zero-order erosion fit for the second stage, respectively. Table 2 summarizes the corresponding model parameters. Fig. 16 shows the overall release profiles for the two films as predicted by the two-stage model. Similar to the PLGA systems, the fit is better for the first stage but not for the plateau at the end of the release.

3.10.3. PLLA membrane release

In contrast to the PLGA and PDLLA films, the PLLA degradation rate is much slower (Fig. 8), as also reported by (Li et al., 1990c). Although the molecular weight decreases dramatically, since degradation occurs primarily in the amorphous regions, degradation of the crystalline region is too low to lead to any significant solubility in the dissolution medium. Moreover, compared with the single-phase dense films for the PLGA and PDLLA films, the PLLA film is highly porous with a honeycomb structure. Consequently, quantification of the release in this system was similar to the approach used with the CA films (Ma and McHugh, 2007). In this case, an effective diffusivity D_{eff} for the porous region is used, where

$$D_{eff} = \frac{D\varepsilon}{\tau} \tag{11}$$

Table 1
Drug release kinetics results for PLGA–acetone membranes with 5% DL.

Sample	a (day^{-1})	b (day^{-2})	R^2 (M_w)	D_0 (cm^2/s)	k_d (h^{-1})	R^2 (k_d)
5% DL, 0% water	0.6935	−0.0458	0.9978	5.68E-13	0.6553	0.9987
5% DL, 5% water	0.3919	−0.0250	0.9957	8.95E-13	0.6785	0.9960

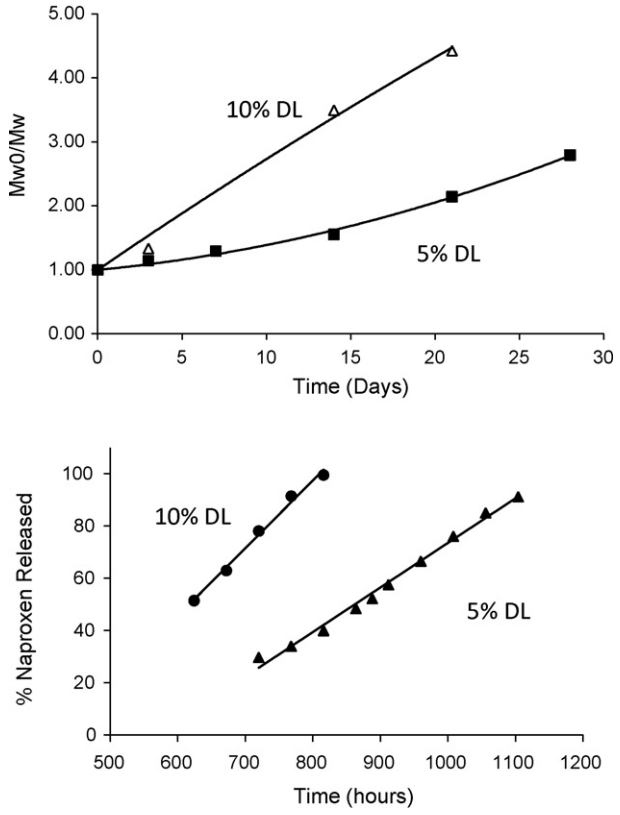

Fig. 15. Plots of model fit with experimental data for PDLLA–acetone films with indicated DL cast from solutions containing 0% water (top — inverse polynomial curve fit for the polymer degradation profiles, bottom — linear plots of release fractions versus time at the second stage of release).

D is the mutual diffusivity of the drug in the amorphous polymer phase, ε is the system overall porosity, and τ is the tortuosity factor for the membrane matrix. The fit to the experimental data is shown in Fig. 17 and the parameter results are summarized in Table 3. Interestingly, the initial effective diffusivity is similar to that for the PDLLA film with the same 5% DL (see Table 2), which has a dense structure. This result is consistent with the findings for the CA films with low DL (Ma and McHugh, 2007). Fig. 17 shows the model prediction for the overall drug release profile assuming no polymer erosion occurs, thus a more-or-less diffusion-controlled parabolic release pattern. The model prediction fits well with the experimental data.

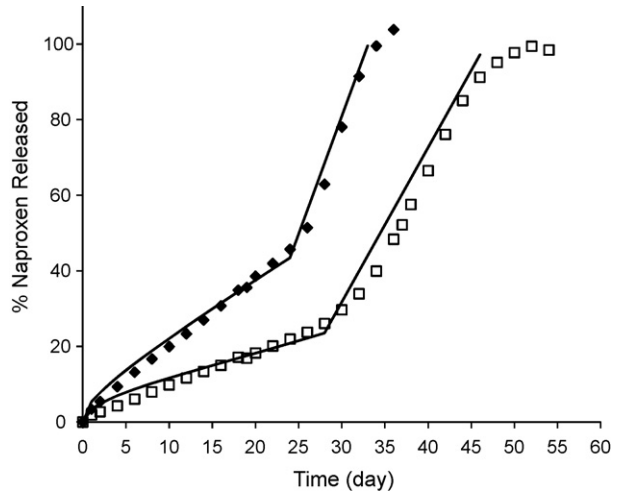

Fig. 16. Plots of model predications and experimental data for PDLLA–acetone films cast from solutions containing 0% water (symbols — experimental data, lines — model predictions). (■) 5% DL; (♦) 10% DL.

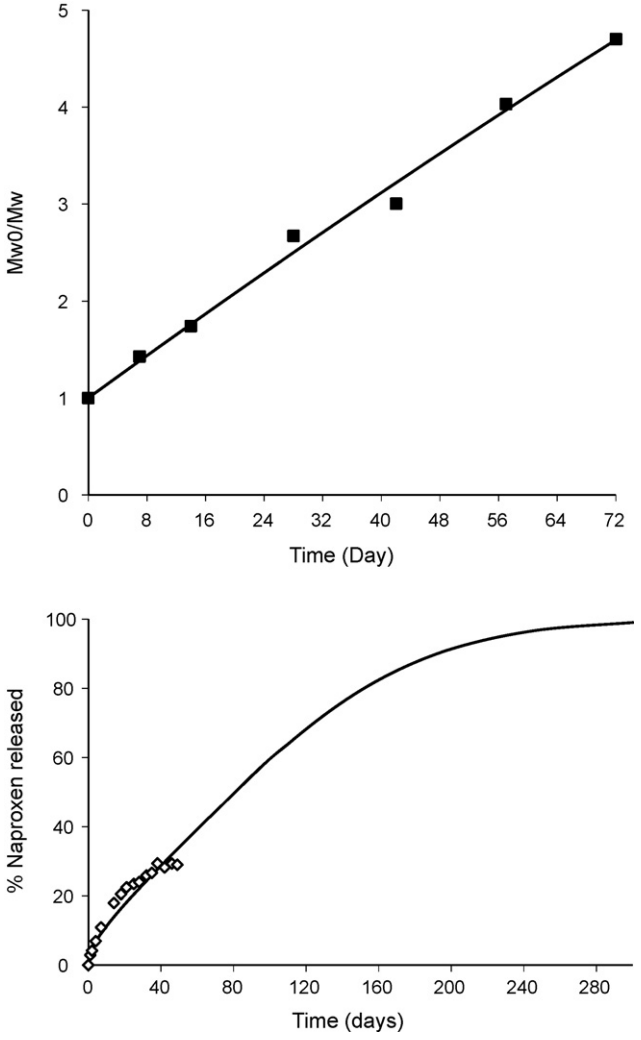

Fig. 17. Plots of model fit and predications with experimental data for 5% DL PLLA-dichloromethane films cast from solutions containing 25% ethanol (top — inverse polynomial curve fit for the polymer degradation profile, bottom — model predictions and experimental data).

Table 3
Drug release kinetics results for PLLA-dichloromethane membranes with 5% DL and 25% ethanol in the casting solution.

Sample	a (day^{-1})	b (day^{-2})	R^2 (M_w)	$D_{eff,0}$ (cm^2/s)
5% DL	0.0550	−5.0E-05	0.9927	4.37E-14

4. Discussion and conclusions

The results described in this paper clearly indicate that the interplay of solution phase inversion and polymer–drug glass transition behavior in cast films with and without crystallization, plays a critical role in the morphology development and locking-in of the structure, and these together profoundly affect the drug release behavior.

For amorphous PLGA and PDLLA membranes cast from acetone 5–8% water solutions with DLs below the solubility limit (0–10% DL), the drug will be dissolved uniformly in the polymer matrix. Although the T_g of the system is only lowered 15–20 °C, locking-

in of the phase-separated morphology is still inhibited due to the intrinsic low T_g of the polymer, i.e. 45 and 55 °C for PLGA and PDLLA, respectively. This is evidenced by the single-phase dense morphologies for the 0% DL films. By contrast, while the T_g of the CA membranes in this DL range is lowered to 150 °C, as much as 40 °C lower than the pure CA membrane (Ma and McHugh, 2007), it is still high enough to lock in the phase-inverted morphology and form a stable honeycomb structure with drug dissolved in the hardened CA-rich phase. At higher drug loadings, up to and beyond the solubility limit (10–40% DL), similar single-phase dense films were obtained for the PDLLA and PLGA films with the precipitated drug particles. Therefore, for PLGA and PDLLA polymers with low T_g, a phase-inverted structure cannot be stabilized by any of the dry casting methods (including free, forced convection, or VIPS) regardless of drug loads. One possible way to obtain phase-separated membranes is through a wet-cast in which the fast solvent–nonsolvent exchange reduces the solvent plasticizing effect and keeps the polymer T_g high enough to lock in the structure during the phase inversion process. Although the wet-cast method is widely used for injectables systems (Brodbeck et al., 1999) and making coated membranes (Herbig et al., 1995), drug loss is likely occurring during the wet casting, especially when the quench bath contains organic solvents. Therefore, this process is not favored for making drug-encapsulated membranes.

For the semi-crystalline PLLA polymers, the membrane morphologies can be better controlled, since the mass transfer path can either pass the s–l demixing line and form a single-phase dense film by polymer crystallization, or the l–l phase-separation and followed by locking-in the two-phase structure by polymer crystallization. However, the relative lack of drug solubility in the crystalline phase leads to unfavorable drug distributions in the film that most often lead to a burst release profile.

Overall, the release rates for PLGA, PDLLA and PLLA membranes were found to follow a two-stage model. Generally, a zero-order desired release is obtained for the second stage in which the release rate is controlled by the polymer erosion. Theoretically, it is also possible to achieve zero-order release by controlling the interplay of polymer degradation rate and drug diffusivity in the membrane through control of the membrane morphology, drug load and distribution in the membrane, as well as drug–polymer interactions.

References

Alexis, F., 2005. Factors affecting the degradation and drug-release mechanism of poly (lactic acid) and poly [(lactic acid-co-(glycolic acid)]. Polym. Int. 54, 36–46.

Bird, R.B., Stewart, W.E., Lightfoot, E.N., 2002. Transport Phenomena, 2nd ed. Wiley, New York, p. 529.

Brodbeck, K.J., DesNoyer, J.R., McHugh, A.J., 1999. Phase inversion dynamics of PLGA solutions related to drug delivery. Part II. The role of solution thermodynamics and bath side mass transfer. J. Control. Rel. 62, 333–344.

Crank, J., 1975. The Mathematics of Diffusion. Oxford, London, pp. 47–48.

Herbig, S.M., Cardinal, J.R., Korsmeyer, R.W., Smith, K.L., 1995. Asymmetric-membrane tablet coatings for osmotic drug delivery. J. Control. Rel. 35, 127–136.

Kumar, N.G., 1980. Viscosity–molecular weight–temperature–shear rate relationships of polymer melts: a literature review. J. Polym. Sci.: Macromol. Rev. 15, 255–325.

Li, S.M., Garreau, H., Vert, M., 1990a. Structure–property relationships in the case of the degradation of massive aliphatic poly (α-hydroxy acids) in aqueous media. Part 1. Poly (DL-lactic acid). J. Mater. Sci.: Mater. Med. 1, 123–130.

Li, S.M., Garreau, H., Vert, M., 1990b. Structure–property relationships in the case of the degradation of massive aliphatic poly (α-hydroxy acids) in aqueous media. Part 2. Degradation of lactide–glycolide copolymers: PLA37. 5GA25 and PLA75GA25. J. Mater. Sci.: Mater. Med. 1, 131–139.

Li, S.M., Garreau, H., Vert, M., 1990c. Structure–property relationships in the case of the degradation of massive aliphatic poly (α-hydroxy acids) in aqueous media. Part 3. Influence of the morphology of poly (L-lactic acid). J. Mater. Sci.: Mater. Med. 1, 198–206.

Li, J., Masso, J.J., Guertin, J.A., 2002. Prediction of drug solubility in an acrylate adhesive based on the drug–polymer interaction parameter and drug solubility in acetonitrile. J. Control. Rel. 83, 211–221.

Liu, H.C., Lee, I.C., Wang, J.H., Yang, S.H., Young, T.H., 2004. Preparation of PLLA membranes with different morphologies. Biomaterials 25, 4047–4056.

Ma, D., McHugh, A.J., 2007. The interplay of phase inversion and membrane formation in the drug release characteristics of a membrane-based delivery system. J. Membr. Sci. 298, 211–290.

Ma, D., 2008. The interplay of drug, polymer and solvent properties in the fabrication of membrane-based delivery systems. Ph.D. Thesis. Lehigh University, Bethlehem, PA.

Mohamed, F., van der Walle, C.F., 2008. Engineering biodegradable polyester particles with specific drug targeting and drug release properties. J. Pharm. Sci. 97, 71–87.

Nair, R., Nyamweya, N., Gönen, S., Martinez-Miranda, L.J., Hoag, S.W., 2001. Influence of various drugs on the glass transition temperature of poly (vinyl pyrrolidone): a thermodynamic and spectroscopic investigation. Int. J. Pharm. 225, 83–96.

Stamatialis, D.F., Papenburg, B.J., Gironĩes, M., Saiful, M.S., Bettahalli, S.N.M., Schmitmeier, S., Wessling, M., 2008. Medical applications of membranes: drug delivery, artificial organs and tissue engineering. J. Membr. Sci. 308, 1–34.

van de Witte, P., Dijkstra, P.J., van den Berg, J.W.A., Feijen, J., 1996a. Phase behavior of polylactides in solvent–nonsolvent mixtures. J. Polym. Sci., Part B: Polym. Phys. 34, 2553–2568.

van de Witte, P., Esselbrugge, H., Dijkstra, P.J., van den Berg, J.W.A., Feijen, J., 1996b. Phase transitions during membrane formation of polylactides. I. A morphological study of membranes obtained from the system polylactide–chloroform–methanol. J. Membr. Sci. 113, 223–236.

Xiang, A., Ma, D., McHugh, A.J., submitted for publication. The role of glass transition and phase inversion in the formation and drug release characteristics of a high T_g biodegradable polymer. J. Membr. Sci.